17,09

Electronic Structure and Optical Properties of Trifluoromethyl Derivatives of C_{60} and C_{70} Fullerenes

© A.I. Murzashev[1], A.P. Zhumanazarov[1], I.E. Kareev[2], V.P. Bubnov[2], A.S. Ryabchikova[1]

[1] Mari State University,
Yoshkar-Ola, Mari El Republic, Russia
[2] Federal Research Center of Problems of Chemical Physics and Medicinal Chemistry RAS,
Chernogolovka, Russia

E-mail: nanotubes59@mail.ru

Received October 19, 2022
Revised November 11, 2022
Accepted November 14, 2022

The energy spectra of ten isomers of trifluoromethyl derivatives of fullerenes $C_{60}(CF_3)_{10}$ and $C_{70}(CF_3)_{10}$ are calculated within the framework of the Hubbard model. Based on the obtained energy spectra, the optical absorption spectra of these compounds are modeled. The calculated optical absorption spectra are compared with the experimental spectra.

Keywords: trifluoromethyl derivatives, fullerene, Hubbard model, energy spectrum, optical absorption spectrum.

DOI: 10.21883/PSS.2023.02.55421.502

1. Introduction

Carbon nanostructures, fullerenes, carbon nanotubes (CNT), and graphenes are among the most demanded materials in terms of their application in various fields of science, industry, biology, health care and many others. Studies show that their electronic properties, which provide for this demand, can be changed in a targeted way by creating compounds with metals and with elements of the halogen group on their basis. The compounds of fullerenes with metals, known as endohedral metal fullerenes, are fullerenes with metal atoms incorporated inside them. The electronic structure of such systems can be described to a good precision by the Hubbard model through adding additional electrons into the electron subsystem of the initial fullerene, valence electrons of the atom incorporated into the fullerene core [1].

In the case of compounds of fullerenes with elements of the halogen group, the situation becomes slightly more complicated. In this case the building up of their energy spectrum can not be only limited by change in the number of electrons in the electron subsystem of the fullerene. This is related to the fact that the connection of these elements to a fullerene is accompanied by formation of bonds between carbon atoms and atom of the connected halogen. The same situation takes place in the case when not a halogen atom is connected to the fullerene, but functional groups based on them, for example, CF_3 groups. In this case the carbon atom of the CF_3 group forms a covalent bond with the carbon atom in the fullerene core. As a result, at the „connection" site the carbon atom, as well as the carbon atom in the CF_3 group, transits to the sp^3 hybridized state, i.e. all valence electrons of these atoms, one s and three p, are „consumed" for the formation of covalent bonds. As a result, there are neither π-electrons nor π-states at the above-mentioned sites. Thus, the $C_n(CF_3)_k$ compounds composed of the C_n fullerene and k groups of CF_3 are a system, where at $n-k$ sites of the fullerene carbon is in the sp^2 hybridized state, and at k sites of the fullerene and k atoms of the CF_3 group it is in the sp^3 hybridized state. Results of [2,3], where $C_{60}(CF_3)_{10}$ and $C_{70}(CF_3)_{10}$ compounds were synthesized, shows that the electronic structure of these system depends significantly on the character of CF_3 groups distribution over the fullerene core. It is clear that systems of $C_n(CF_3)_{10}$ type, as well as compounds of C_nG_k type, where G being an element of the halogen group, are promising in terms of creation of compounds with pre-defined electronic properties on their basis.

Thus, studying electronic properties of $C_n(CF_3)_k$ type compounds is an actual task in terms of practical application and theoretical research. This work is devoted to theoretical study of electronic and optical properties of $C_{60}(CF_3)_{10}$ and $C_{70}(CF_3)_{10}$ isomers that have been synthesized, structurally and spectrometrically characterized in [2,3].

2. Model and method

In fullerenes carbon is in sp^2 hybridized state. Three valence electrons of carbon form hard covalent bonds between the carbon atoms that form the system core, while the fourth non-hybrid electron, remaining partly free, due to the overlapping of wavefunctions between the sites forms a π-electron subsystem. The boundary between vacant and occupied states of electrons in such systems lays in the region of these particular electrons. As a result, all electronic and optical properties of fullerenes, as well as those of CNTs and graphenes, are formed by processes in this π-electron

subsystem. As for the electron states that form the core of the system of σ-electrons, the states of these electrons are about 20 eV below the states of π-electrons [4]. That is, π-electron states of fullerenes and other systems similar to them are responsible for their electronic and optical properties, while states of σ-electrons are responsible for their structural stability.

Main processes that form the structure of the π-electron subsystem are the processes of their hopping from one site to another. Until recently the electronic structure of carbon nanosystems with sp^2 hybridization has been studied within the models based on the above-mentioned fact. It was assumed that the integral of π-electrons hopping between neighboring sites is $B \approx -2.6$ eV. However, in 2011 in [5], it was shown by ab initio calculations that carbon systems with sp^2-hybridization are characterized by strong intrasite Coulomb interaction (ISCI) of π-electrons, which can be as high as ~ 10 eV. This circumstance requires a system description within the Hubbard model [6].

The Hubbard model is easy-to-view, its Hamiltonian has the following form:

$$H = \varepsilon \sum_{i,\sigma} n_{i,\sigma} + B \sum_{i,j\neq i,\sigma} (a^+_{i\sigma} a_{j\sigma} + a^+_{j\sigma} a_{i\sigma}) U \sum_{i,\sigma} n_{i,\uparrow} n_{i,\downarrow}. \quad (1)$$

In (1) ε — electron self-energy, U — Coulomb interaction energy at one site, B — integral of hopping between neighbor sites, $n_{i,\sigma} = a^+_{i,\sigma} a_{i,\sigma}$ — particle number operator in the i-th site with spin σ, $a^+_{i\pi}$ and a_{is} — operators of electron creation and annihilation, respectively, with spin σ at the i-th site. The first term in (1) is self-energy of π-electrons, the second term describes the contribution of their hopping between neighbor sites, the third term is their Coulomb interaction at one site. Summation over i is performed over all sites of the system, and summation over j in the second term is performed over the sites that are neighboring to the site i. In the sites, where carbon is in the sp^3 hybridized state, there are no π-states and π-electrons. Therefore all summations over i and j for systems of $C_n(CF_3)_k$ type in (1) must be performed over the sites, excluding those where carbon is in the sp^3 state, that is excluding the sites where the trifluoromethyl group is located.

In our works [7–10] we have suggested a static fluctuation approximation (SFA) to calculate energy spectra of fullerenes and other carbon nanosystems. Within the framework of this approximation the energy levels can be determined as Fourier transform poles of the anticommutator Green's function $G_{i\sigma}(\tau) \langle\langle a^+_{i\sigma}(\tau) | a_{i\sigma(0)} \rangle\rangle \equiv \langle [a^+_{i\sigma}(\tau), a_{i\sigma}]_+ \rangle$. Here $a^+_{i\sigma}(\tau)$ is creation operator in the Heisenberg representation

$$a^+_{i\sigma}(\tau) = e^{\hat{H}\tau} a^+_{i\sigma}(0) e^{-\hat{H}\tau}, \quad (2)$$

$a^+_{i\sigma}(0)$ — particle creation operator in the Schroedinger representation at the i-th site of the lattice with a spin projection of $\sigma = \{\uparrow\downarrow\}$, and $\tau = it$ is imaginary Matsubara time. The successive application of SFA results in the following: each energy level of the π-electron subsystem is split into two levels: the first level corresponds to the state when one π-electron with an arbitrary spin orientation is at the site, the second level corresponds to the state when two electrons with opposite spins are at the site. As a result, the subsystem of π-electrons is split into two groups of levels, the „upper" and „lower" Hubbard subbands. States of the lower Hubbard subband correspond to the states with single-occupation of sites by electrons, while the upper subband corresponds to double-occupation of sites. The „lower" Hubbard subband is fully occupied, while the „upper" subband is fully vacant. It should be noted, that each energy level with a degeneracy of m is occupied not by $2m$ electrons with pairwise opposite spins, m electrons with $\uparrow$ spin and m electrons with $\downarrow$ spin, but by m electrons with arbitrary spin orientation. Energy levels of the „upper" Hubbard subband can be represented as $E_k + U/2$, while those of the „lower" subband — as $E_k - U/2$ [7–10]. In these studies it was shown that for carbon nanosystems with sp^2 hybridization parameters of the Hubbard model must be as follows: $B \approx -1$ eV, $U \approx 7.0$ eV. To determine them, it is necessary to solve the following system of linear differential equations

$$\frac{d\bar{a}_{k\sigma}(\tau)}{d\tau} = \varepsilon_k \bar{a}^+_{k\sigma}(\tau) + B \sum_{j\neq k} \bar{a}^+_{j\sigma}(\tau) \quad (3)$$

with initial conditions: $\bar{a}_\sigma(\tau)|_{I=0} = a^+_{k\sigma}$, where $a^+_{k\sigma}$ is creation operator in the Schroedinger representation. In (3), k numbers the system sites where carbon is in the sp^2 hybridized state and summation over j covers the sites that are neighboring to k. as commonly known, the solution to system (3) has the following form:

$$\bar{a}^+_{k\sigma}(\tau) = \sum_{k=1}^{Q} M_k e^{E_k \tau}. \quad (4)$$

In [7–10] it is shown that numbers M_k represent degeneracy degree of a level, Q is quantity of levels, and the energy levels themselves, as was already mentioned, are sets of two bands with level energies of $\{E_k + U/2\}$ and $\{E_k - U/2\}$.

It should be stressed, that in case of a fullerene without functional groups or other carbon nanosystem composed of carbon atoms in the sp^2 hybridized state only, (3) is a system of N equations, where N is the number of atoms in the system. In the case of $C_n(CF_3)_k$ and C_nG_k type compounds, where G being an element of the halogen group, the number of equations in system (3) will be equal to $n - k$, which is evident, because the number of sp^2 hybridized carbon atoms in such systems is equal exactly to $n - k$. In this case the summation over $j \neq k$ in the second term of the right part of (3) also must be performed

only over the sites with sp^2 hybridization, i.e. over the sites without CF_3 groups.

With known energy spectrum of the system and rules of selection for optical (dipole) transitions, the optical absorption spectrum (OAS) is calculated by the following formula according to [11]:

$$In(\omega) \sim \sum M_k M_n \delta\left(\hbar\omega - \left(\tilde{E}_n - \tilde{E}_k\right)\right), \qquad (5)$$

here the summation over n and k is performed over the states between which transitions are permitted by the selection rules, M_k, M_n are degeneracy degrees of the states, and $\delta(x)$ is the Dirac delta function. It's worth noting that in equation (5) $\tilde{E}_k$ correspond to occupied states (glqq the lower Hubbard subband"), and $\tilde{E}_n$ correspond to vacant states („the upper Hubbard subband"). For specific calculations it is convenient to take the Dirac delta function in its approximated representation:

$$\delta(x) = \frac{1}{\pi} \lim_{\gamma \to 0} \frac{\gamma}{x^2 + \gamma^2}. \qquad (6)$$

If γ in (6) is taken as a phenomenological parameter equal to attenuation of π-states due to the processes not taken into account in our model, we get a formula for the absorption intensity:

$$In(\omega) \sim \sum_{k,n} \frac{\gamma M_k m_n}{(\omega - \Delta E)^2 + \gamma^2}. \qquad (7)$$

3. Energy spectrum and optical absorption spectrum of compounds $C_{60}(CF_3)_{10}$

In [2] authors have synthesized, structurally and spectroscopically characterized five compounds of the $C_{60}(CF_3)_{10}$ composition that were different in the pattern of distribution of trifluoromethyl groups on the surface of fullerene core. The authors have performed quantum-chemical calculations of the compounds in question by the DFT method and prognosed values of the HOMO-LUMO gap between vacant and occupied states. In addition, OASes of produced compounds were measured. The analysis of results reported in [2] shows, that electronic and optical characteristics of the studied compounds depend significantly on the pattern of distribution of CF_3 groups over sites of the fullerene core. To investigate the effect of the pattern of functional groups distribution on electronic properties of compounds, we used the technique of [1] within the Hubbard model to calculate the energy spectrum of five $C_{60}(CF_3)_{10}$ isomers synthesized in [2], that were different from each other by mutual arrangement of trifluoromethyl groups on the fullerene surface. In [2] these isomers are named as C60-10-1, C60-10-2, C60-10-3, C60-10-4, and C60-10-5, their Schlegel diagrams are shown in Fig. 1.

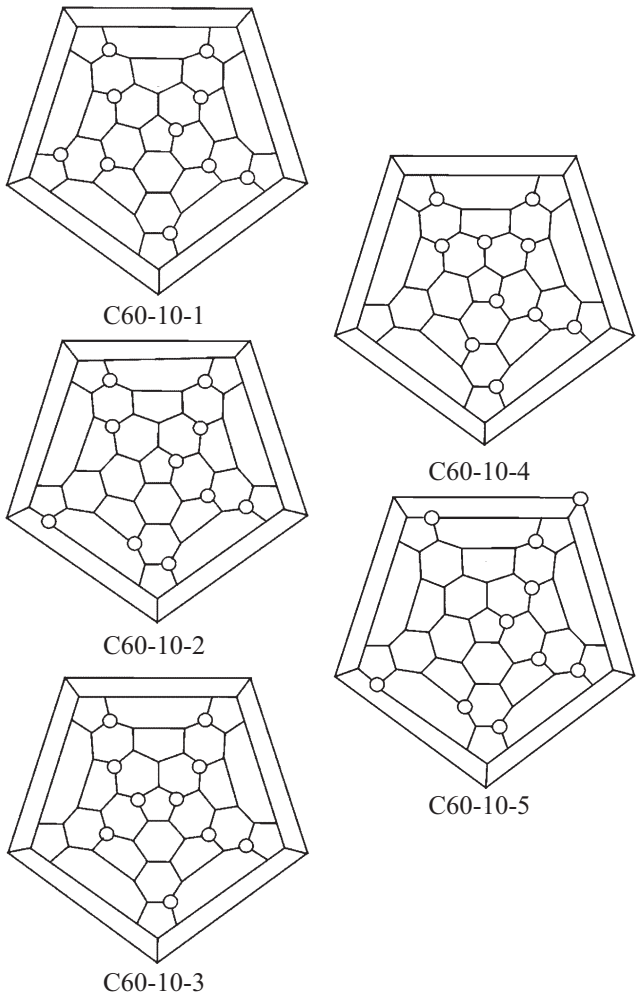

Figure 1. Schlegel diagrams for isomers of C_{60} fullerene with ten trifluoromethyl groups, large circles indicate sites where CF_3 groups are located.

The difference in electronic structure of these systems is clearly shown by their OASes presented in Fig. 2–6 (the upper graph „*a*"). Despite the identical composition, their OASes defined by the energy spectrum of the π-electron subsystem are considerably different, as can be seen from the graphs. It is clear that energy spectra of the π-electron subsystem of above-mentioned isomers depend significantly on the pattern of CF_3 groups distribution over the fullerene surface. Based on this, to study the pattern of the effect of CF_3 groups distribution on the energy spectrum of systems in question, we have calculated energy spectra and OASes of C60-10-1, C60-10-2, C60-10-3, C60-10-4, and C60-10-5 isomers.

For this purpose, according to the technique described in the previous section, energy spectra of these systems were calculated. Parameters of the Hubbard model were taken from the considerations to have as close as possible match between the OAS curves of isomers and the experimental curves. Now we shall present briefly the main characteristics

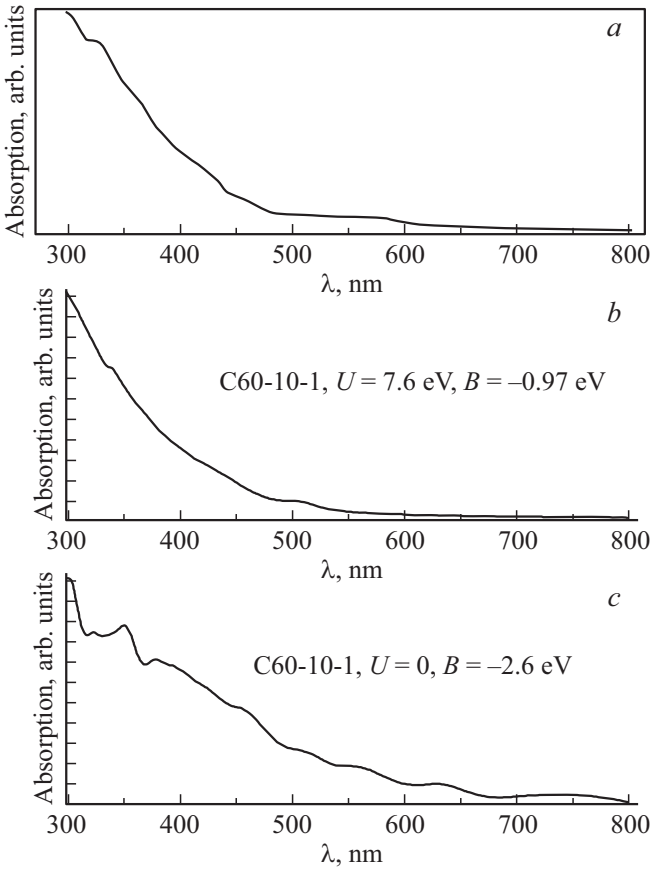

Figure 2. OAS curves of C60-10-1 isomer. The upper graph is an experimental curve measured in [2], in the middle — a theoretical curve for the following parameters of the Hubbard model: $U = 7.6$ eV, $B = -0.97$ eV, the lower graph is a theoretical curve obtained within the model without taking into account the intrasite Coulomb interaction.

of the obtained energy spectra and OAS curves of above-mentioned compounds.

The energy spectrum of C60-10-1 isomer fullerene is composed of 96 levels, of which four levels are double-degenerate, other levels are non-degenerate. With parameters of the Hubbard model equal to $U = 7.6$ eV, $B = -0.97$ eV, width of each Hubbard subband is $W \approx 5.16$ eV, the HOMO-LUMO gap is $\Delta \approx 2.44$ eV. The HOMO-LUMO gap is 1.75 times greater than the predicted value of 1.39 eV obtained in [2] on the basis of DFT-calculations (PBE functional and TZ2P basis) (see Table 4 in [2]). At the same time, the gap width calculated by us matches the absorption edge wavelength $\lambda_{max} \sim 665$ nm obtained for the C60-10-1 isomer in [2]. This, to our opinion, is indicative of incorrectness of the DFT method use in [2] for the calculation of the energy spectrum of systems under study.

The energy spectrum of C60-10-2 isomer contains 96 levels, of which 4 levels are double-degenerate, other levels are non-degenerate. With parameters of the Hubbard model equal to $U = 7.3$ eV, $B = -1.0$ eV, width of each Hubbard subband is $W \approx 5.2$ eV, the HOMO-LUMO gap is $\Delta \approx 2.00$ eV. The gap value, as is the case for the C60-10-1 isomer, is considerably greater than the value of 1.550 eV obtained in [2] through DFT-calculations (Table 4 in [2]) and matches quite well the value of absorption edge wavelength $\lambda_{max} \sim 610$ nm obtained for this isomer in [2].

The energy spectrum of C60-10-3 isomer contains 98 levels, of which 2 levels are double-degenerate, other levels are non-degenerate. With parameters of the Hubbard model equal to $U = 7.99$ eV, $B = -1.0$ eV, width of Hubbard subbands is $W \approx 5.37$ eV, the HOMO-LUMO gap is $\Delta \approx 2.62$ eV. The value, as is the case for two previous isomers, is considerably greater than the value of 1.662 eV predicted in [2] through DFT-calculations (Table 4 in [2]) and matches well the value of absorption edge wavelength $\lambda_{max} \sim 540$ nm for this isomer in [2].

The energy spectrum of C60-10-4 isomer contains 90 levels, of which 10 levels are double-degenerate, other levels are non-degenerate. With parameters of

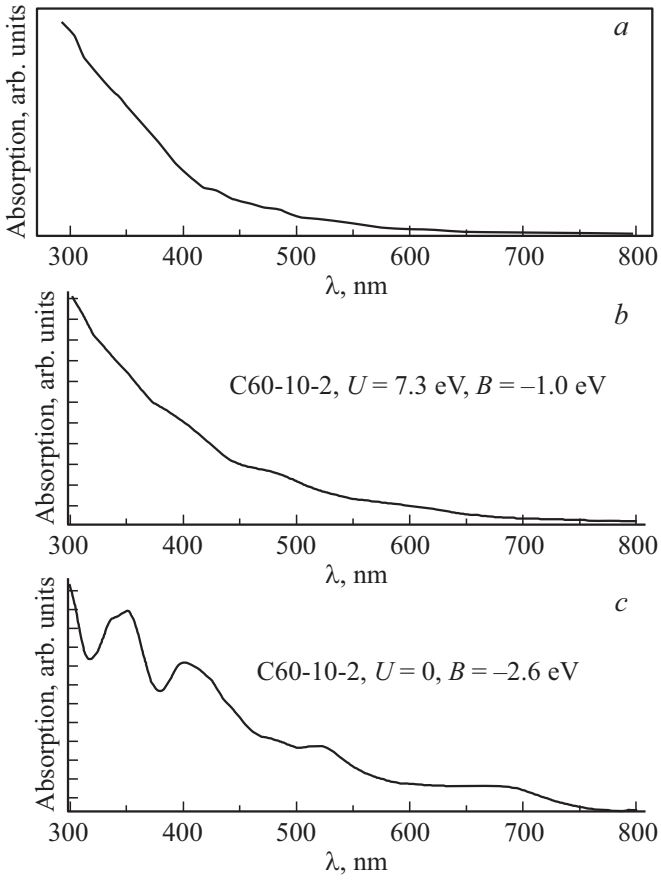

Figure 3. OAS curves of C60-10-2 isomer. The upper graph is an experimental curve measured in [2], in the middle — a theoretical curve for the following parameters of the Hubbard model: $U = 7.3$ eV, $B = -1.0$ eV, the lower graph is a theoretical curve obtained within the model without taking into account the intrasite Coulomb interaction.

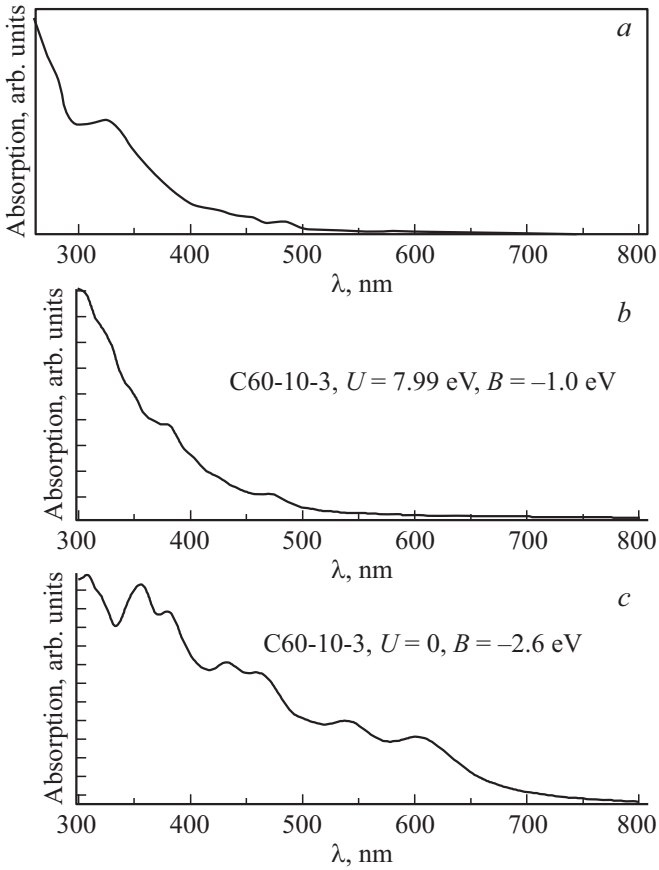

Figure 4. OAS curves of C60-10-3 isomer. The upper graph is an experimental curve measured in [2], in the middle — a theoretical curve for the following parameters of the Hubbard model: $U = 7.99$ eV, $B = -1.0$ eV, the lower graph is a theoretical curve obtained within the model without taking into account the intrasite Coulomb interaction.

the Hubbard model equal to $U = 7.9$ eV, $B = -1.0$ eV, width of Hubbard subbands is $W \approx 5.40$ eV, the HOMO-LUMO gap is $\Delta \approx 1.504$ eV. This gap value is slightly different from 1.636 eV predicted by DFT-calculations [2] (Table 4 in [2]) and matches well the value of absorption edge wavelength $\lambda_{\max} \sim 610$ nm for this isomer in [2].

The energy spectrum of C60-10-5 isomer is composed of 82 levels, of which 2 levels are six-fold degenerate, another 2 levels are five-fold degenerate, other levels are non-degenerate. With parameters of the Hubbard model equal to $U = 7.9$ eV, $B = -1.0$ eV, width of Hubbard subbands is $W \approx 5.33$ eV, the HOMO-LUMO gap is $\Delta \approx 2.57$ eV. This value is different from 1.748 eV predicted by DFT-calculations [2] (Table 4 in [2]) and matches quite well the value of absorption edge wavelength $\lambda_{\max} \sim 550$ nm for this isomer in [2].

Optical absorption spectra of the investigated isomers are shown in Fig. 2–6. The upper graph in these figures marked as „*a*“ is an experimental curve measured in [2], below it these is the OAS calculated within our model, which is marked as „*b*“ and takes into account the intrasite Coulomb interaction of π-electrons, with indication of parameters of the Hubbard model. It can be seen from the graphs, that patterns of the absorption intensity dependence on wavelength of the experimental curves (a) and theoretical curves obtained with ISCI taken into account (b) match each other at a good qualitative level. Here it is also worth noting, that such important characteristic of OAS as the experimentally obtained absorption edge matches well both the theoretical values and the HOMO-LUMO value for all curves, which is indicative of correctness of the model used by us. The lower curves („*c*“) in Fig. 2–6 represent OASes of corresponding isomers calculated without taking ISCI into account, at hopping integral values of $B = -2.6$ eV. In can be seen from the figures, that OAS curves obtained without taking ISCI into consideration do not match the experimental curves, which is indicative of the need to take ISCI into account when studying electronic and optical properties of fullerenes and their derivatives.

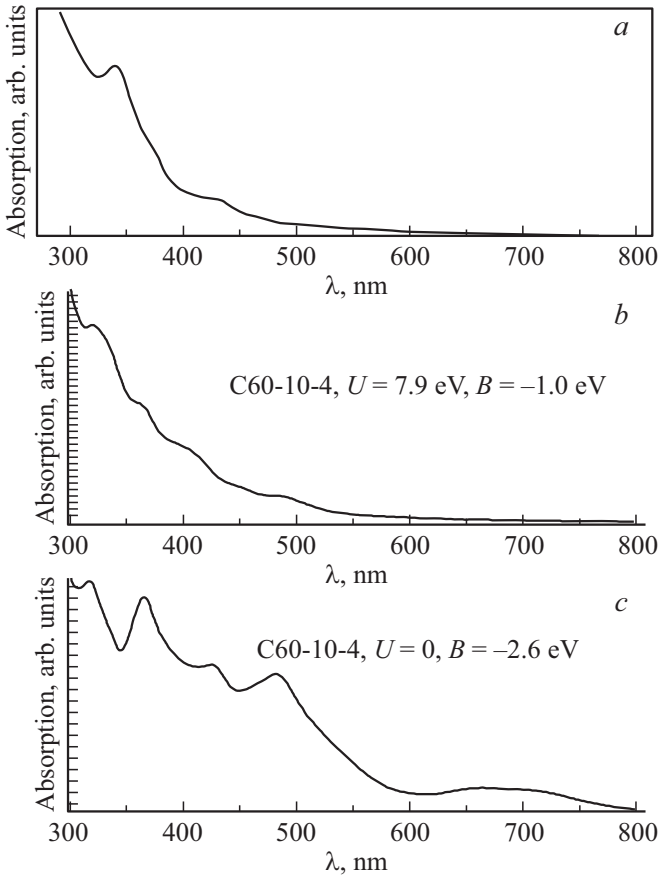

Figure 5. OAS curves of C60-10-4 isomer. The upper graph is an experimental curve measured in [2], in the middle — a theoretical curve for the following parameters of the Hubbard model: $U = 7.9$ eV, $B = -1.0$ eV, the lower graph is a theoretical curve obtained within the model without taking into account the intrasite Coulomb interaction.

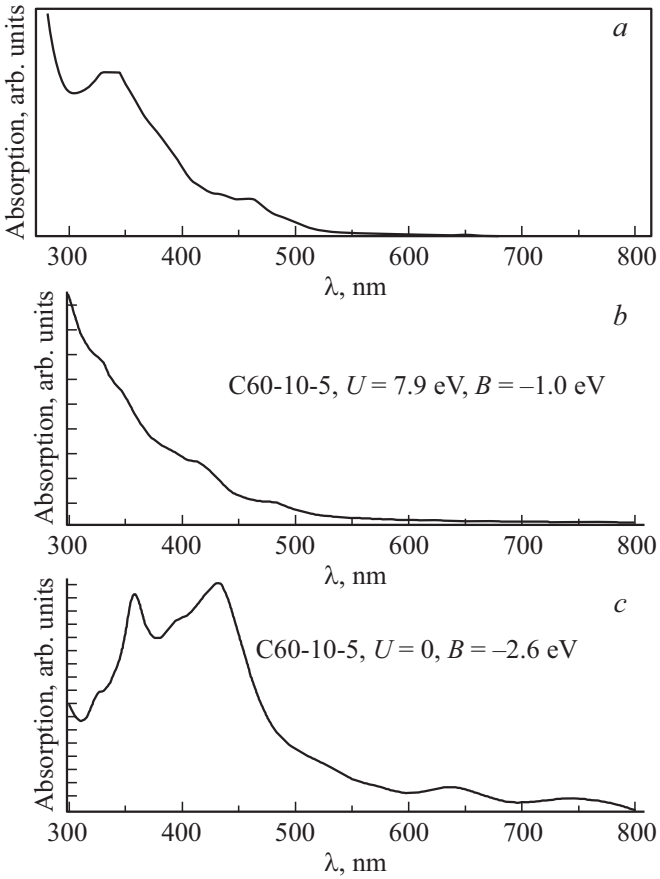

Figure 6. OAS curves of C60-10-5 isomer. The upper graph is an experimental curve measured in [2], in the middle — a theoretical curve for the following parameters of the Hubbard model: $U = 7.9$ eV, $B = -1.0$ eV, the lower graph is a theoretical curve obtained within the model without taking into account the intrasite Coulomb interaction.

4. Energy spectrum and optical absorption spectrum of compounds $C_{70}(CF_3)_{10}$

In [3] authors have synthesized, structurally and spectroscopically characterized five isomers of trifluoromethyl derivative $C_{70}(CF_3)_{10}$. The analysis of results reported in this study, as well as in [2], shows, that electronic properties of the studied systems depend significantly on the pattern of distribution of trifluoromethyl groups over the fullerene core of C_{70}. As it is in the case of $C_{60}(CF_3)_{10}$, this is clearly shown by the significant difference in OASes of $C_{70}(CF_3)_{10}$ isomers that have in their composition 10 trifluoromethyl groups, various isomers of which in [3] are named as C70-10-1, C70-10-2, C70-10-3, C70-10-4, C70-10-5. Schlegel diagrams of these isomers are shown in Fig. 7. In this context, as it is for $C_{60}(CF_3)_{10}$ compounds, it is necessary to calculate energy spectra of $C_{70}(CF_3)_{10}$ systems, which structures are represented by Schlegel diagrams in Fig. 7.

Also, we have calculated energy spectra of C70-10-1, C70-10-2, C70-10-3, C70-10-4, C70-10-5. Parameters of the Hubbard model for the calculation were taken from the considerations to have as close as possible match between the OAS curves calculated on the basis of the presented energy spectra and the experimental curves measured in [3]. OAS curves of C70-10-1, C70-10-2, C70-10-3, C70-10-4, C70-10-5 isomers are shown in Fig. 8–12.

The energy spectrum of C70-10-1 isomer is composed of 118 levels. Among them 2 levels are double-degenerate, other levels are non-degenerate. With parameters of the Hubbard model equal to $U = 7.65$ eV, $B = -0.95$ eV, width of Hubbard subbands is $W \approx 5.12$ eV, the HOMO-LUMO gap is $\Delta \approx 2.53$ eV. The gap value is significantly different from 1.3620 eV obtained in [3] through DFT-calculations (Table 1 in [3]). The gap value of 2.53 eV matches the absorption edge wavelength equal to $\lambda_{max} \approx 491$ nm.

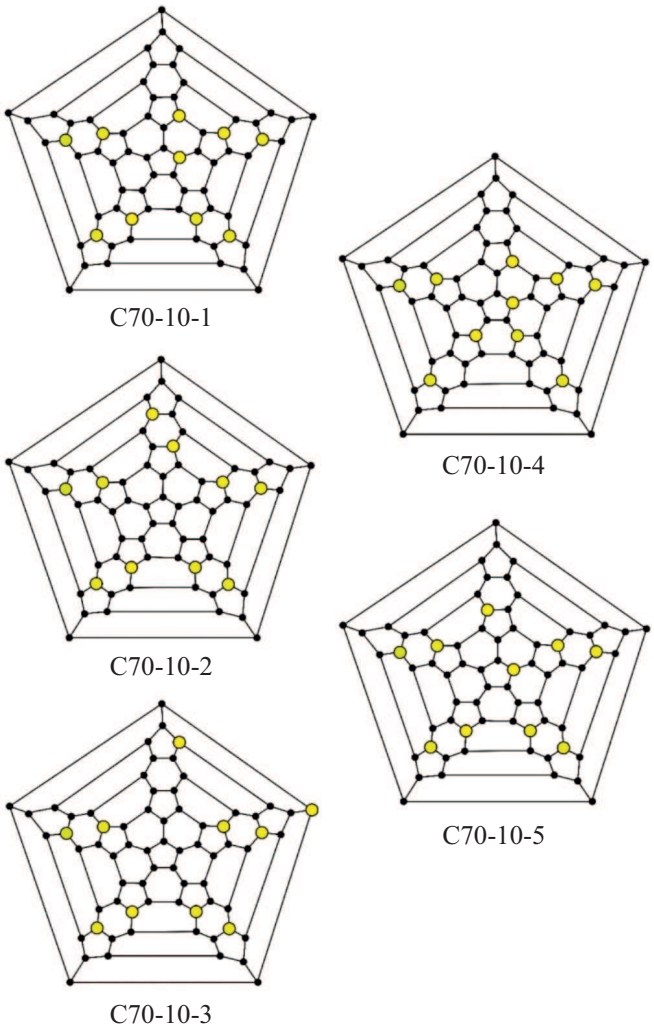

Figure 7. Schlegel diagrams of isomers of C_{70} fullerene with ten trifluoromethyl groups, large circles indicate sites where CF_3 groups are located.

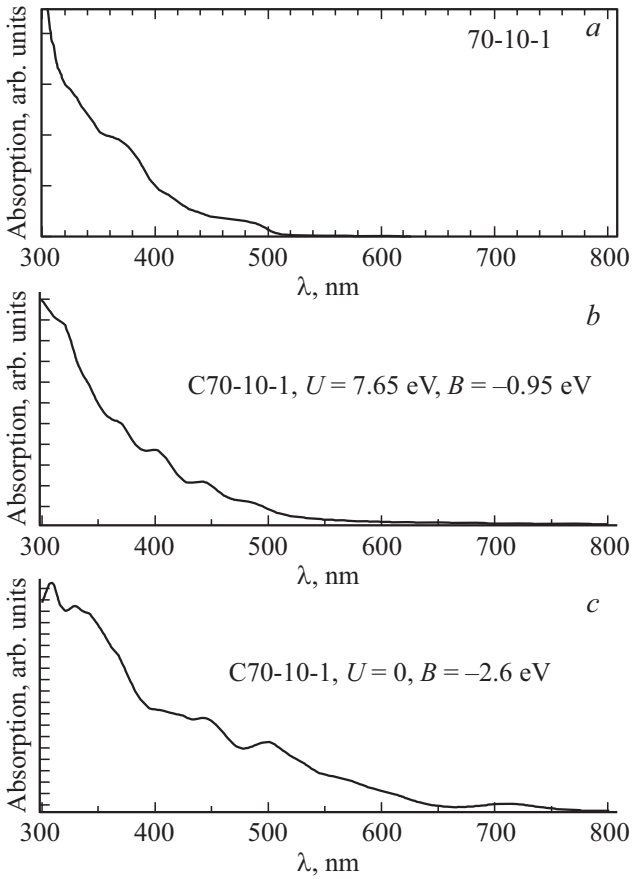

Figure 8. OAS curves of C70-10-1 isomer. The upper graph is an experimental curve measured in [3], in the middle — a theoretical curve for the following parameters of the Hubbard model: $U = 7.65$ eV, $B = -0.95$ eV, the lower graph is a theoretical curve obtained within the model without taking into account the intrasite Coulomb interaction.

The energy spectrum of C70-10-2 isomer contains 112 levels, of which 4 levels are three-fold degenerate, other levels are non-degenerate. With parameters of the Hubbard model equal to $U = 7.27$ eV, $B = -0.91$ eV, width of Hubbard subbands is $W \approx 4.82$ eV, the HOMO-LUMO gap is $\Delta \approx 2.45$ eV. The gap value is significantly different from 1.823 eV obtained in [3] through DFT-calculations (Table 1 in [3]). The gap value of 2.45 eV matches the absorption edge wavelength equal to $\lambda_{max} \approx 508$ nm.

The energy spectrum of C70-10-3 isomer contains 118 levels, of which 2 levels are double-degenerate, other levels are non-degenerate. With parameters of the Hubbard model equal to $U = 7.27$ eV, $B = -0.91$ eV, width of Hubbard subbands is $W \approx 4.88$ eV, the HOMO-LUMO gap is $\Delta \approx 2.39$ eV. The gap value is significantly different from 1.679 eV obtained in [3] through DFT-calculations (Table 1 in [3]). The gap value of 2.39 eV matches the absorption edge wavelength equal to $\lambda_{max} \approx 520$ nm.

The energy spectrum of C70-10-4 isomer contains 118 levels, of which 2 levels are double-degenerate, other levels are non-degenerate. With parameters of the Hubbard model equal to $U = 7.0$ eV, $B = -1.0$ eV, width of Hubbard subbands is $W \approx 5.41$ eV, the HOMO-LUMO gap is $\Delta \approx 1.59$ eV. The gap value is slightly different from 1.628 eV obtained in [3] through DFT-calculations (Table 1 in [3]). The gap value of 1.59 eV matches the absorption edge wavelength equal to $\lambda_{max} \approx 782$ nm.

The energy spectrum of C70-10-5 isomer contains 116 levels, of which 4 levels are double-degenerate, other levels are non-degenerate. With parameters of the Hubbard model equal to $U = 7.25$ eV, $B = -0.98$ eV, width of Hubbard subbands is $W \approx 5.25$ eV, the HOMO-LUMO gap is $\Delta \approx 2.00$ eV. The gap value is significantly different from 1.370 eV obtained in [3] through DFT-calculations (Table 1 in [3]). The gap value of 2.00 eV matches the absorption edge wavelength equal to $\lambda_{max} \approx 622$ nm.

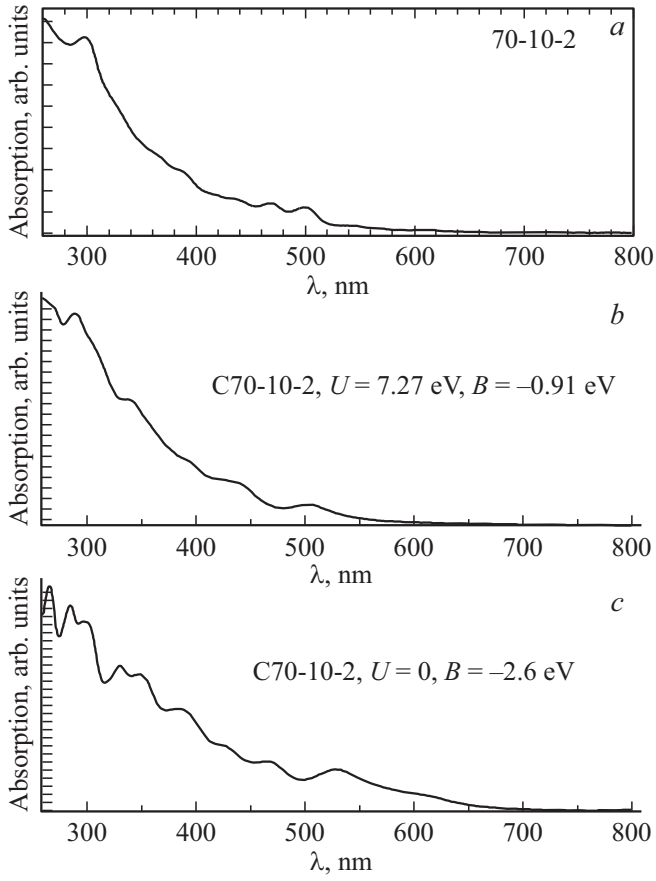

Figure 9. OAS curves of C70-10-2 isomer. The upper graph is an experimental curve measured in [3], in the middle — a theoretical curve for the following parameters of the Hubbard model: $U = 7.27$ eV, $B = -0.91$ eV, the lower graph is a theoretical curve obtained within the model without taking into account the intrasite Coulomb interaction.

Optical absorption spectra of the investigated isomers are shown in Fig. 8–12. The upper graph marked as „*a*“ is an experimental curve measured in [3], below it these is a curve of absorption intensity dependence on wavelength calculated within our model taking into account the intrasite Coulomb interaction of π-electrons, with indication of parameters of the Hubbard model; this curve is marked as „*b*“. It can be seen from the graphs, that patterns of the absorption intensity dependence on wavelength of the experimental curves (a) and theoretical curves obtained with ISCI taken into account (b) match each other at a good qualitative level. The lower curves („*c*“) in Fig. 8–12 represent OASes of investigated isomers calculated without taking ISCI into account, at hopping integral values of $B = -2.6$ eV. It can be seen from the figures, that for C70-10-1, C70-10-2, C70-10-3, C70-10-4, C70-10-5 isomers, as well as for C60-10-1, C60-10-2, C60-10-3, C60-10-4, C60-10-5 isomers the OAS curves obtained without taking ISCI into account do not match the experimental curves. The obtained results are indicative of the need to take ISCI into account when studying electronic and optical properties of fullerenes and their derivatives.

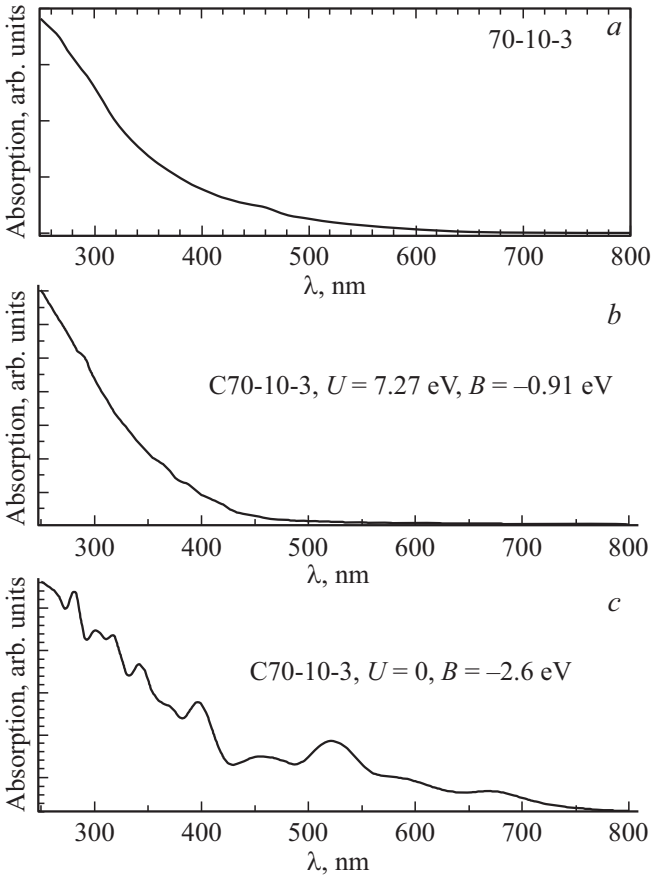

Figure 10. OAS curves of C70-10-3 isomer. The upper graph is an experimental curve measured in [3], in the middle — a theoretical curve for the following parameters of the Hubbard model: $U = 7.27$ eV, $B = -0.91$ eV, the lower graph is a theoretical curve obtained within the model without taking into account the intrasite Coulomb interaction.

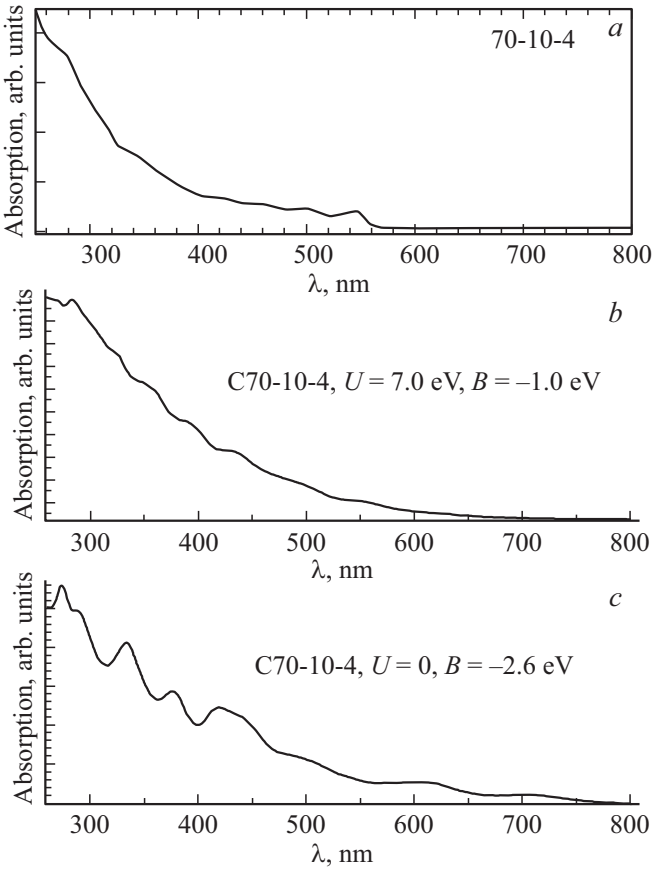

Figure 11. OAS curves of C70-10-4 isomer. The upper graph is an experimental curve measured in [3], in the middle — a theoretical curve for the following parameters of the Hubbard model: $U = 7.0$ eV, $B = -1.0$ eV, the lower graph is a theoretical curve obtained within the model without taking into account the intrasite Coulomb interaction.

5. Conclusion

The comparison between the experimental optical absorption spectra and the optical absorption spectra of five $C_{60}(CF_3)_{10}$ isomers of trifluoromethyl derivatives and five $C_{70}(CF_3)_{10}$ isomers modelled on the basis of energy spectra of these compounds by the Hubbard method taking into account the intrasite Coulomb interaction of π-electrons at one site has shown that the match each other at a good qualitative level. The obtained results unambiguously demonstrate that it is necessary to take into account the intrasite Coulomb interaction when modelling electronic and optical properties of fullerene derivatives. Also, the HOMO-LUMO gaps calculated by the Hubbard method for ten investigated compounds have shown a good match with absorption edge values of the investigated compounds, as opposed to the correspondent values obtained through DFT-calculations (PBE functional

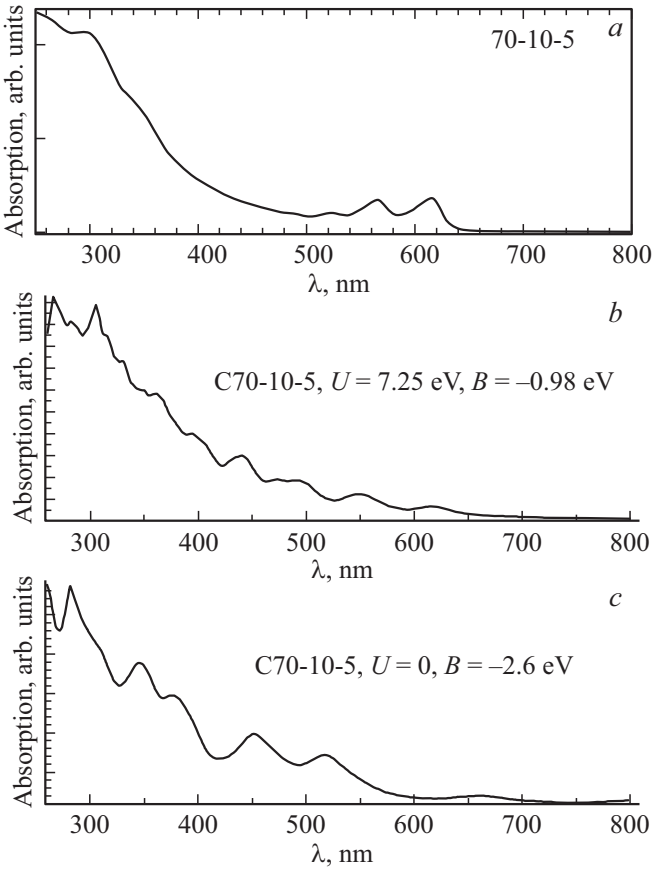

Figure 12. OAS curves of C70-10-5 isomer. The upper graph is an experimental curve measured in [3], in the middle — a theoretical curve for the following parameters of the Hubbard model: $U = 7.25$ eV, $B = -0.98$ eV, the lower graph is a theoretical curve obtained within the model without taking into account the intrasite Coulomb interaction.

and TZ2P basis). This is indicative of the fact that the use of the Hubbard model is more correct for the description of trifluoromethyl derivatives of C_{60} and C_{70} fullerenes.

Funding

The work has been carried out under the State Assignment subject, state registration No. AAAA-A19-119092390079-8.

Conflict of interest

The authors declare that they have no conflict of interest.

References

[1] V.P. Bubnov, I.Ye. Kareev, B.V. Lobanov, A.I. Murzashev, V.M. Nekrasov, FTT **58**, *8*, 1639 (2016) (in Russian).
[2] A.A. Popov, I.E. Kareev, N.B. Shustova, E.B. Stukalin, S.F. Lebedkin, K. Seppelt, S.H. Strauss, O.V. Boltalina, L. Dunsch. J. Am. Chem. Sos. **129**, *37*, 11551 (2007).
[3] A.A. Popov, I.E. Kareev, N.B. Shustova, S.F. Lebedkin, S.H. Strauss, O.V. Boltalina, L. Dunsch. Chem. Eur. J. **14**, *1*, 107 (2008).
[4] A.A. Levin, Vvedeniye v kvantovuyu khimiyu tvyordogo tela, Khimiya, M. (1974). 238 p. (in Russian).
[5] T.O. Wehling, E. Sasıoglu, C. Friedrich, A.I. Lichtenstein, M.I. Katsnelson, S. Blü gel. Phys. Rev. Lett. **106**, *23*, 236805 (2011).
[6] J. Hubbard. Proc. Roy. Soc. **276**, 238 (1963).
[7] G.I. Mironov, A.I. Murzashev, FTT **53**, *11*, 2273 (2011) (in Russian).
[8] A.I. Murzashev, E.O. Shadrin, ZhETF **145**, *6*, 1161 (2014) (in Russian).
[9] A.I. Murzashev, T.E. Nazarova, ZhETF **146**, *5*, 1026 (2014) (in Russian).
[10] A.I. Murzashev, FTT **62**, *3*, 484 (2020) (in Russian).
[11] L.D. Landau, E.M. Lifshitz. Teoreticheskaya fizika, FIZMATLIT, M. (2002). V. 3. 804 p. (in Russian).

Translated by Ego Translating